

Industrial water reclamation using polymeric membranes – case studies involving a car manufacturer and a beverage producer

Bernard A. Agana, Darrell Reeve and John D. Orbell

ABSTRACT

This study presents the evaluation of different polymeric membranes for the reclamation of wastewater generated by two manufacturers. Specifically, ultrafiltration (UF) membranes were evaluated for wastewater pretreatment use while nanofiltration (NF) and reverse osmosis (RO) membranes were evaluated for wastewater reclamation use. Results show that both the UF membranes used were not suitable for pretreatment of the oily wastewater stream due to the presence of suspended cathodic electrodeposition (CED) paint particles. The CED paint particles rapidly deposit on the membrane surface resulting in severe fouling and very low permeate fluxes. With respect to the metals and beverage wastewater streams, the polyvinylidene-difluoride (PVDF) UF membrane was shown to be more suitable for pretreatment than the polyacrylonitrile UF membrane. The PVDF-UF membrane had relatively lower flux decline rates, higher turbidity and higher total organic carbon reduction rates. Meanwhile, the low-pressure RO membrane proved to be suitable for wastewater reclamation of the oily and beverage wastewater streams – showing low flux decline rates, high conductivity and high chemical oxygen demand reduction rates. In terms of reclaiming the metals wastewater stream, the NF membrane proved more suitable than the low-pressure RO membrane. The NF membrane had relatively higher permeate fluxes and metals rejection rates compared to the RO membrane.

Key words | cross-flow velocity, nanofiltration, polymeric membrane, reverse osmosis, transmembrane pressure, ultrafiltration

Bernard A. Agana
John D. Orbell (corresponding author)
School of Engineering and Science,
Victoria University,
PO Box 14428,
Melbourne,
Victoria 8001,
Australia
E-mail: John.Orbell@vu.edu.au

Darrell Reeve
John D. Orbell
Institute for Sustainability and Innovation,
Victoria University,
PO Box 14428,
Melbourne,
Victoria 8001,
Australia

INTRODUCTION

A number of researchers have shown that certain types of membrane can be used to treat the various wastewaters generated during car manufacturing and beverage production. For example, it was shown in our previous work (Agana *et al.* 2011, 2012) that a 50 nm ceramic ultrafiltration (UF) membrane can be used to recover wastewater generated at a car manufacturer's post-electrodeposition rinsing stage. Likewise, Anderson *et al.* (1981) showed that a cellulose acetate reverse osmosis (RO) membrane can work successfully in reclaiming wastewater generated from an automotive electrocoat painting process. In terms of beverage production, Tay & Jeyaseelan (1995) demonstrated the viability of a combined UF and RO treatment system in

the reclamation of bottle-washing wastewater. They concluded that the combined UF and RO system not only reduces freshwater consumption but also conserves energy.

Membranes have also been shown to work successfully in treating similar wastewater streams generated by different production facilities. For example, in an experiment involving the treatment of vegetable-oil-contaminated factory wastewater, using a polysulfone UF membrane (Mohammadi & Esmaeilifar 2004), reductions in water quality parameters such as chemical oxygen demand (COD), total organic carbon (TOC), total suspended solids and phosphate concentration exceeded 85%. Similarly, good retention rates for emulsified solvent and oil and grease

were obtained when a cellulose acetate UF membrane was used for treatment of spent solvent rinses from nickel-plating operations (Qin *et al.* 2004). The retention rates for emulsified solvent and oil and grease were reported to be 96 and 80%, respectively.

Although a number of investigations have been carried out on the membrane treatment of wastewater generated by car manufacturing and beverage production processes individually, to the best of our knowledge, no work has been carried out that compares the suitability of identified membranes in reclaiming wastewater generated by these contrasting large industries.

The work described in this paper aimed to determine the suitability of selected polymeric membranes (UF, nanofiltration (NF) and RO) for the reclamation of wastewater generated at the production facilities of a car manufacturer and a beverage producer. Wastewater streams generated at these production facilities have substantial volumes – making wastewater reclamation desirable in order to reduce excessive water consumption. The suitability of the selected membranes was evaluated based on reduction/rejection rates in relation to critical water quality parameters, permeate flux decline rates and power usage. Likewise, to visualize the degree of fouling on the membrane surface, fouled membranes were analysed using a field emission scanning electron microscope (FESEM). In general, the UF membranes were evaluated for pretreatment of wastewater whilst the NF and RO membranes were evaluated for wastewater reclamation.

METHODS

Wastewater samples

Actual wastewater samples were obtained from a car manufacturer and a beverage producer operating in the western suburbs of Melbourne, Australia. The samples were collected in 20 L containers and kept in a cold room at a temperature of 4 °C. Prior to every experiment, a specified sample volume is transferred into a stainless steel container. The container is then left for a couple of hours inside the laboratory to bring up the wastewater temperature to ambient level. All samples were used within 48 hours of collection.

UF membranes

Two types of polymeric flat sheet UF membranes, supplied by GE Osmonics, were used in the experiments – namely, JW (polyvinylidene-difluoride) membrane with molecular weight cut-off (MWCO) of 30 kD (pore size: 3.25 nm) and MW (polyacrylonitrile) membrane with MWCO of 100 kD (pore size: 10 nm). The JW membrane is hydrophobic (contact angle: 66°) and the MW membrane is extremely hydrophilic (contact angle: 4°). UF membranes used for experiments were soaked in deionized water overnight to remove any surface impurities.

NF and RO membranes

Both the NF (DL series) and low-pressure RO (AK series) membranes used in the experiments were supplied by GE Osmonics. The NF membrane is a thin-film membrane having an approximate MWCO of 0.15–0.30 kD for uncharged organic molecules. Similar to the NF membrane, the RO membrane is also a thin-film membrane having high flux and a NaCl rejection rate of approximately 99.0%. The NF membrane was specifically tested on the metals wastewater sample and the RO membrane was tested on all the wastewater samples.

NF and RO membranes preparation

All NF and RO membranes used in the experiments were soaked in deionized water overnight to remove any surface impurities. Prior to using the NF and RO membranes, a wetting protocol was followed (Mänttari *et al.* 2002; Jezowska *et al.* 2006). In this case, deionized water having an average conductivity of 2 $\mu\text{S cm}^{-1}$ was pumped into the membrane for 15 min. The pressure and temperature of the deionized water was maintained at 2.5 MPa and 25 °C respectively throughout the wetting period.

Membrane filtration system

A schematic diagram of the membrane filtration system used in the experiments is shown in Figure 1. A variable speed pump with ½ hp motor was used to deliver wastewater into the flat sheet test cell (Sterlitech CF 042 Development

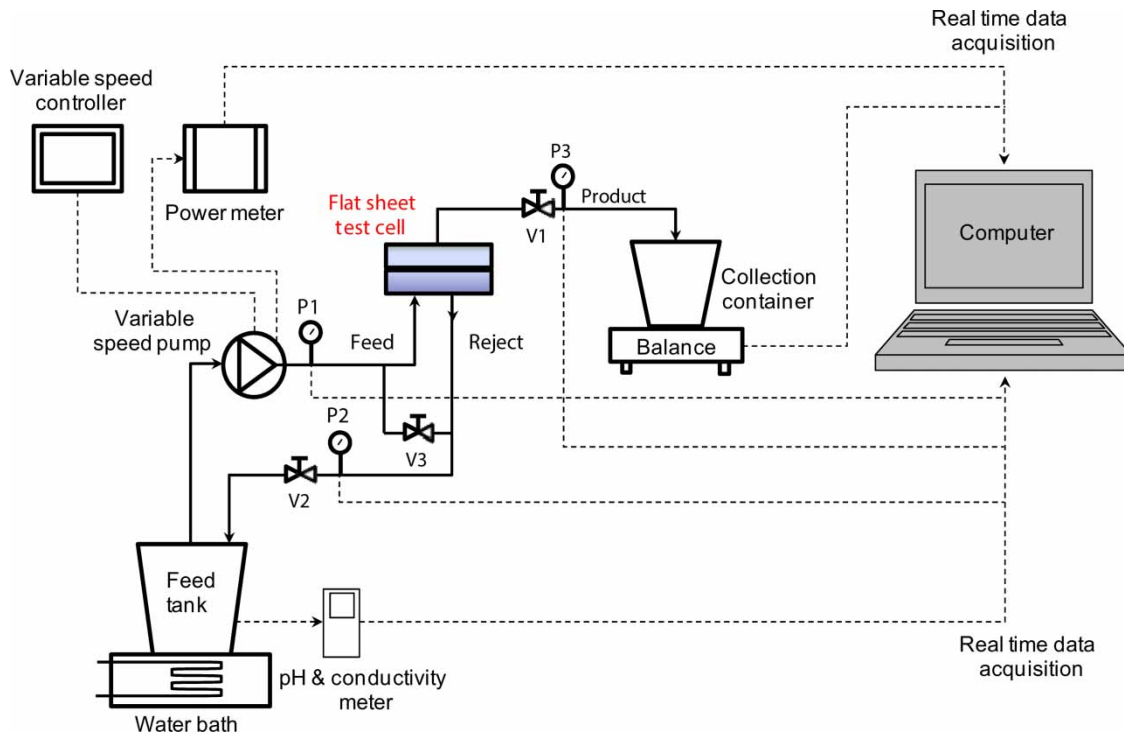


Figure 1 | Schematic diagram of the laboratory-scale membrane filtration system used in the experiments. P: pressure gauge; V: valve. Solid lines represent water flow while broken lines represent real time data acquisition.

Cell). Membrane permeate was collected into a container and weighed and reject water was returned into the feed tank to facilitate increase of feed water concentration and fast track the rate of membrane fouling. The feed tank was submerged halfway into a water bath to maintain the temperature within a specified range. Operating parameters such as power usage, pressures, temperatures, weights and water qualities (pH and conductivity) were monitored at set intervals using probes and recorders connected to a computer.

UF experiments

Wastewater samples collected were directly used as feed into the UF membranes. Experiments were carried out at a cross-flow velocity (CFV) of 2.4 m s^{-1} and at transmembrane pressures (TMPs) of 0.2 and 0.4 MPa. The temperature range during the experiments was maintained within $19\text{--}24^\circ\text{C}$. Operating parameters previously mentioned were continuously monitored at 15 min intervals. Samples of feedwater and membrane permeate were collected into containers and sent to a NATA (National

Association of Testing Authorities) accredited laboratory for analysis on water quality parameters such as oil & grease (O&G) and TOC. In addition, feedwater and membrane permeate turbidity were measured during the experiments to estimate suspended particle rejection rates. The volume of wastewater sample used for each experiment is 6 L while filtration area for all UF membranes used is 0.0042 m^2 . Each experimental run lasted for approximately 6 hours.

NF and RO experiments

Prior to actual experiments, wastewater samples collected were filtered through a $0.3 \mu\text{m}$ filter to remove any suspended particles present. Both the NF and RO membrane experiments were carried out at a CFV of 2.7 m s^{-1} and at TMPs of 0.69, 1.03 and 1.38 MPa. The temperature range during the experiments was maintained within $25\text{--}29^\circ\text{C}$. Operating parameters previously mentioned were continuously monitored at 5 min intervals. Similar to the UF experiments, samples of feedwater and membrane permeate

were collected into containers and sent to a NATA accredited laboratory for analysis on water quality parameters such as COD, conductivity and metals content. The volume of filtered wastewater sample used in each experiment was 3 L while filtration area for both the NF and RO membranes was 0.0042 m². Each experiment run lasted for approximately 2 hours.

Analytical methods

The size distribution and zeta potential (ζ) of particles in the actual wastewater samples were measured using a Malvern Zetasizer Nano Series (Nano-ZS). Turbidity measurements were carried out using a La Motte 2020 Series Turbidity Meter. The reduction/rejection rates (% P_R) of the critical water quality parameters previously mentioned were calculated using Equation (1):

$$\%P_R = [(P_F - P_P)/P_F] \times 100\% \quad (1)$$

where P_F is the parameter concentration in the feedwater (mg L⁻¹) and P_P is the parameter concentration in the membrane permeate (mg L⁻¹).

After each experiment, used membranes were washed with deionized water and air dried at ambient temperature. Representative portions of each air-dried membranes were cut (approximately 1 cm²) and mounted on aluminum stubs with carbon tape. They were then coated with a layer of gold and analysed under a FESEM (Philips XL30 FEG).

RESULTS AND DISCUSSION

Pure water flux

Experiments aimed at establishing the relationship between pure water flux (PWF) and TMP were carried out prior to commencing actual wastewater experiments. Distilled water (conductivity of 2 μ S cm⁻¹) was used as feed to ensure that no form of fouling will occur during filtration. Results showed that PWFs of the polymeric membranes were highly correlated ($R^2 > 0.99$) with TMP as shown in Figures 2(a) and 2(b). A high correlation between PWF

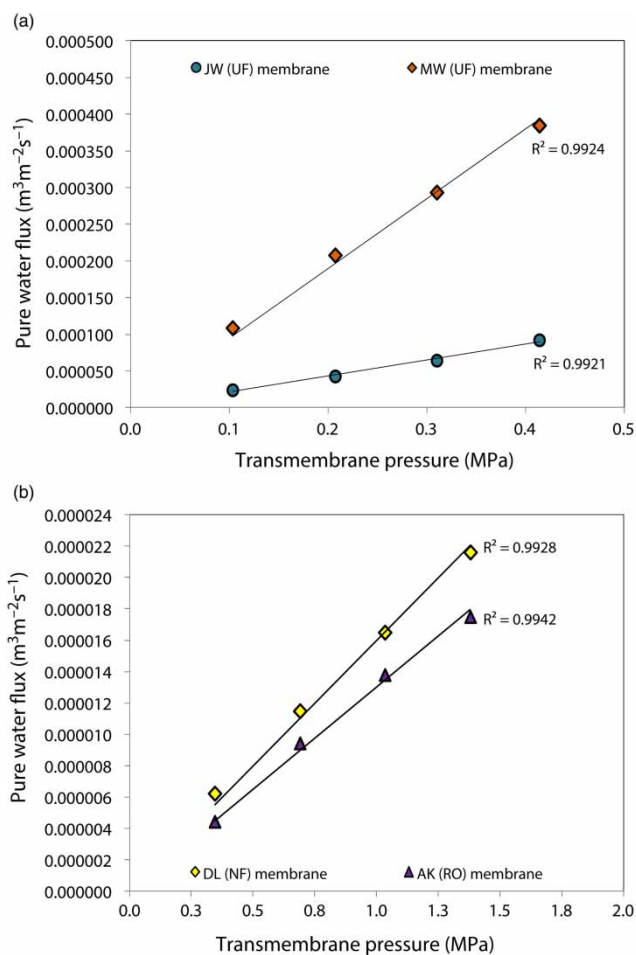


Figure 2 | Pure water fluxes of (a) UF membranes as a function of TMP at a CFV of 2.4 m s⁻¹ and standard temperature of 20 °C and (b) NF and RO membranes as a function of TMP at a CFV of 2.7 m s⁻¹ and standard temperature of 25 °C.

and TMP is expected since the only resistance present during the experiments is the intrinsic membrane resistance. The slopes of the line shown in Figures 2(a) and 2(b) give the pure water permeabilities of the membranes.

Figure 2(a) shows that the PWF of the MW membrane was higher than the JW membrane. The disparity between the PWFs of the two UF membranes can be attributed to the relative membrane structure and properties (i.e. hydrophilicity/hydrophobicity). For example, the MW membrane was designed to be extremely hydrophilic and it might be expected to have higher water fluxes than the hydrophobic JW membrane. This scenario is similar to the PWFs obtained for NF and RO membranes (Figure 2(b)). An NF membrane has relatively looser pores compared to an RO membrane and is expected to have a higher PWF.

Characteristics of wastewater samples

The particle size distributions for the wastewater samples collected are shown in Figure 3. The oily and metals wastewater samples obtained from the car manufacturer have particle sizes ranging from 90 to 532 nm (mean diameter 245.5 nm) and 18 to 397 nm (mean diameter 134.1 nm) respectively. In contrast, wastewater samples from the beverage producer have particle sizes in the range of 24 to 5,560 nm (mean diameter 161.4 nm).

The average ζ of the particles present in the wastewater samples collected are shown in Table 1. The values of ζ for both the metals and beverage production wastewater samples suggest that the particles present have incipient instability (ASTM 1985), and thus particle aggregation may occur. Particle aggregation is not considered to be a problem during UF because the more the particles aggregate, the better. Larger particles have higher hydrodynamic forces acting on them and therefore are more likely to be swept away from the membrane surface. In contrast, the ζ of particles found in the oily wastewater sample suggests that the particles have good

stability and are well dispersed in solution, thus aggregation is unlikely to happen. In this particular case, the particle sizes present in the oily wastewater sample can be assumed to be the same throughout the experiments. Therefore, the possibility for the finer suspended particles to deposit on the membrane surface is high.

The typical characteristics of the wastewater samples used in the experiments are shown in Table 2.

UF experiments

Permeate fluxes (J , $\text{m}^3 \text{m}^{-2} \text{s}^{-1}$) were calculated using Equation (2):

$$J = (0.001 \times W) / (A_M \times t) \quad (2)$$

where W is the weight measured by the balance (kg), A_M is the effective membrane area (m^2), t is the sampling time (s). To account for temperature variations, all permeate fluxes were standardized at a temperature of 20 °C using Equation (3) (Crittenden et al. 2005):

$$J_{20^\circ\text{C}} = J(1.03)^{TS-TM} \quad (3)$$

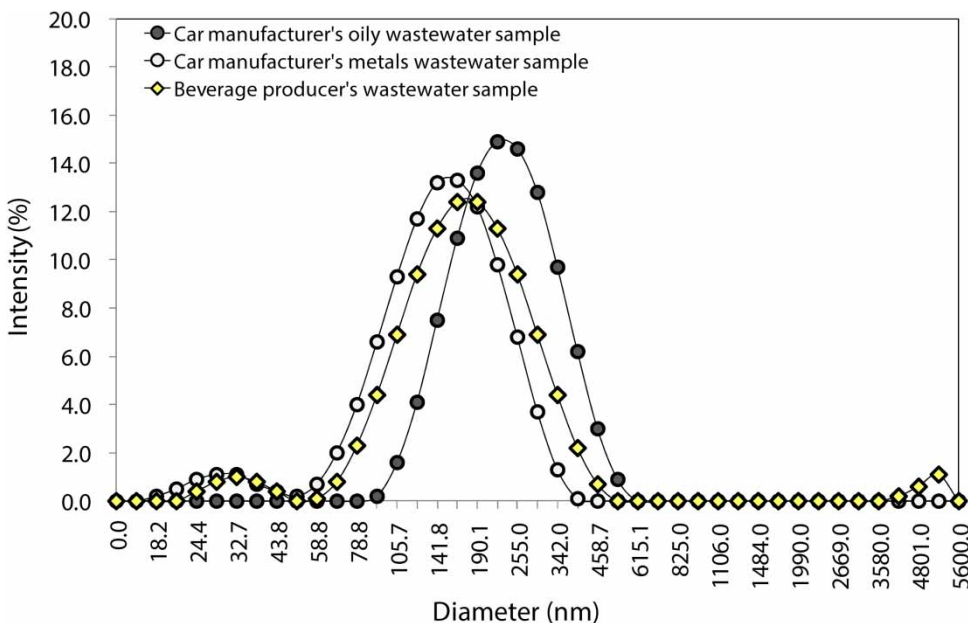


Figure 3 | Particle size distributions for wastewater samples used in the experiments.

Table 1 | Average ζ of particles found in the wastewater samples

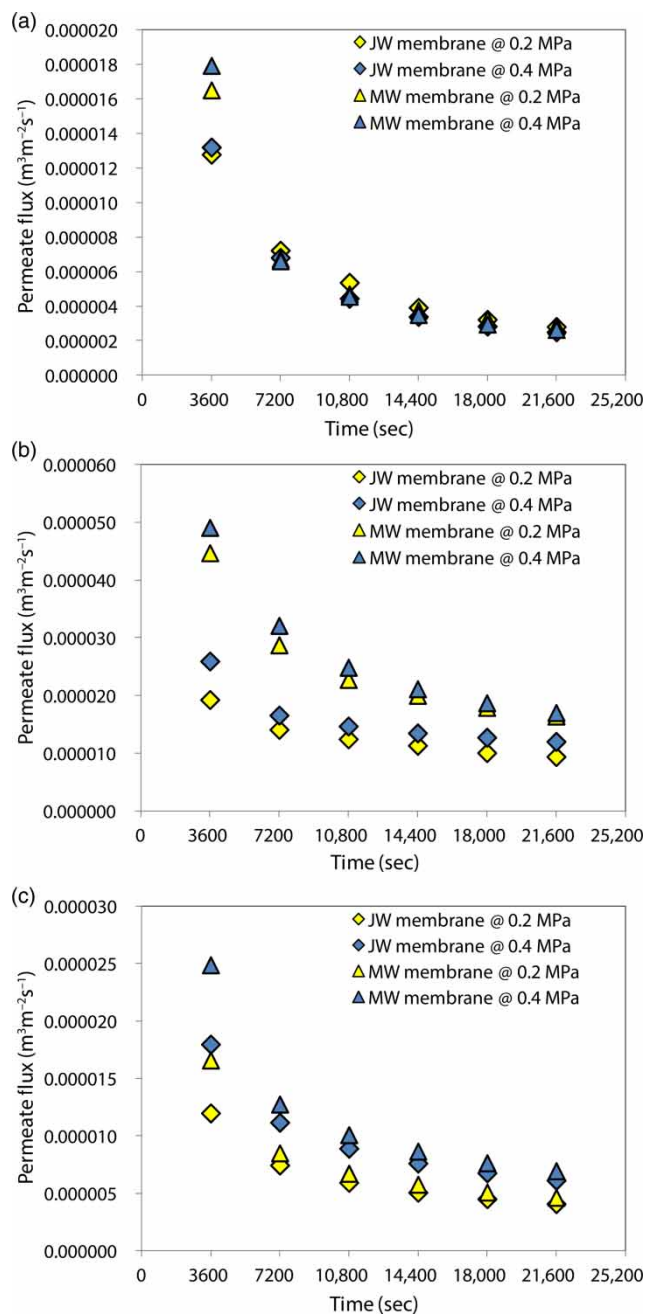
Wastewater sample	pH	Particle ζ
Car manufacturer's oily wastewater sample	7.5	56 ± 2 mV
Car manufacturer's metals wastewater sample	3.8	-21 ± 2 mV
Beverage producer's wastewater sample	8.3	-23 ± 2 mV

Table 2 | Typical characteristics of wastewater samples used in the experiments

Water quality parameters	Oily wastewater sample	Metals wastewater sample	Beverage production wastewater sample
pH	7.5	3.8	8.3
Conductivity ($\mu\text{S cm}^{-1}$)	979	1,579	1,129
COD (mg L^{-1})	230	91	4,900
O&G (mg L^{-1})	21	<5	17
TOC (mg L^{-1})	120	16	140
Turbidity (NTU)	294	43	58
Colour	Light gray	Hazy white	Murky, yellowish
Phosphorus (P, mg L^{-1})	5	71	–
Iron (Fe, mg L^{-1})	1.13	4	–
Manganese, Mn (mg L^{-1})	0.06	23	–
Nickel (Ni; mg L^{-1})	0.02	40	–
Zinc (Zn; mg L^{-1})	1.23	98	–

where $J_{20^\circ\text{C}}$ is the flux at a standard temperature of 20°C ($\text{m}^3 \text{m}^{-2} \text{s}^{-1}$), T_S is the standard temperature (20°C), T_M is the measured temperature ($^\circ\text{C}$).

Both the JW and MW membranes showed the same flux decline profiles when tested on the oily wastewater sample (Figure 4(a)). A rapid decline in flux was observed for 2 hours followed by a gradual decline throughout the remainder of the experimental run. Of the two membranes tested for this wastewater sample, the MW membrane showed the worst flux decline rates at all TMPs used, which can be explained by considering the membrane's permeability. As noted previously, the pure water permeability of the MW membrane is significantly higher than for the JW membrane (Figure 2(a)). Howe *et al.* (2007) showed that membranes with higher permeability fouled faster than membranes with lower permeability. Membranes with higher permeability have bigger pores compared to those with lower permeability. Initially, membranes with bigger pores will

**Figure 4** | Permeate fluxes obtained for JW and MW membranes: (a) oily wastewater sample; (b) metals wastewater sample; (c) beverage production wastewater sample.

have higher fluxes but once particles start to deposit on the pores, fluxes obtained will drastically be reduced until such time that the pore openings have become smaller. Consequently, the smaller pore openings will inhibit further deposition of particles – resulting in gradual flux decline.

Fouling rates during experiments using the oily wastewater sample were greatly influenced by the presence of suspended cathodic electrodeposition (CED) paint particles. These particles include paint pigment, unstable resins and polymers. Positively charged CED paint particles deposit rapidly on the surfaces of the JW and MW membranes. The combination of membrane surface-particle interaction and applied TMP resulted in intense fouling of both membranes. Fouling mechanisms observed during the oily wastewater experiments include intermediate pore blocking and cake layer formation. Intermediate pore blocking occurred during the first two hours of the experiments resulting in rapid flux decline (Figure 4(a)). Subsequently, cake layer formation was the prevailing fouling mechanism. Deposition of paint particles happened initially on the membrane pores and was followed by accumulation of particles on the membrane surface, resulting in cake layer formation. Fouling of the MW membrane was more severe than for the JW membrane because it has larger pore sizes and higher surface porosity, as shown in Figures 5(a) and 5(b). Aside from membrane structure, charge attraction can also be a contributing factor in the rapid deposition of CED paint particles on the pores and surface of the MW membrane. Since the CED paint particles are positively charged (Streitberger 2007), they are attracted to the negatively charged surface of the MW membrane. The MW membrane was modified by its manufacturer to become extremely hydrophilic (GEC 2010). Such membrane modification usually involves the partial hydrolysis of the membrane material with NaOH –

resulting in improved hydrophilicity and a negative surface charge (Wang et al. 2007).

The degree of deposition of CED paint particles on the surfaces of the JW and MW membranes are shown in Figures 6(a) and 6(b). As previously mentioned, surface-particle interaction and applied TMP resulted in intense fouling of the membranes. During the UF of the oily wastewater sample, CED paint particles continuously deposit on the membrane surface. The particles that have already deposited on the membrane surface are then compressed leading to higher cake resistance and low permeate flux. The reduction of permeate flux is further magnified at higher TMPs as shown in Figure 4(a). Higher pressures cause the cake layer on the membrane surface to compress further, resulting in a much lower permeate flux.

Comparing the three different kinds of wastewater stream, the JW and MW membranes performed better for the metals wastewater sample (car manufacturer), as shown in Figure 4(b) – with a relatively higher permeate flux being achieved for both membranes. This was particularly noticeable for the MW membrane which achieved steady-state permeate fluxes of approximately 0.000016 and $0.000017 \text{ m}^3 \text{ m}^{-2} \text{ s}^{-1}$ at TMPs of 0.2 and 0.4 MPa respectively. However, although the MW membrane had higher permeate fluxes, its flux decline rates were relatively higher than for the JW membrane – as shown in Figure 4(b). This suggests that a JW membrane may be more suitable for the metals wastewater sample than the MW membrane. The higher flux decline rates experienced by the MW membrane is a sign of intense fouling. A membrane intensely fouled

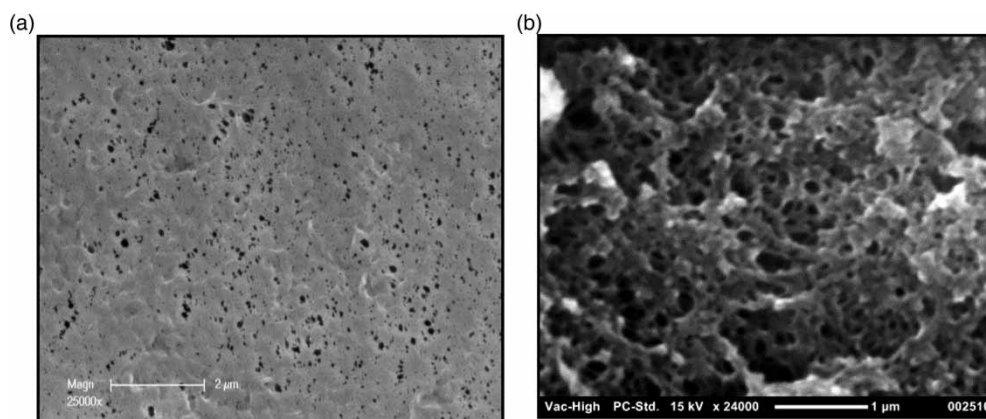


Figure 5 | Surface structures of fresh (a) JW and (b) MW membranes.

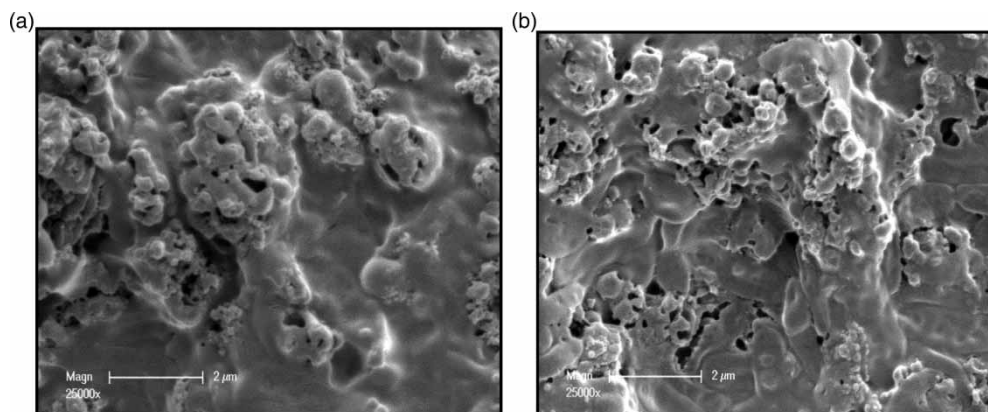


Figure 6 | Surface images of (a) JW and (b) MW membranes used for oily wastewater sample.

may require longer cleaning time and the use of aggressive chemicals in order to be regenerated. Such a scenario may lead to premature membrane material degradation and shorter lifespan.

The relatively improved performance of both membranes for the metals wastewater sample can be attributed to the instability of the particles present in this wastewater. As mentioned previously, the instability of the suspended particles will promote aggregation. It may be argued that because particles present in the metals wastewater sample have a tendency to aggregate, the cake layers formed on the surfaces of both membranes (Figures 7(a) and 7(b)) were more porous compared to the cake layers formed in experiments on the oily wastewater sample. Likewise, the dominant fouling mechanism during the experiments can be deduced to be cake layer formation.

Improvement in permeate fluxes for both the JW and MW membranes in experiments using the beverage production wastewater were not significant compared to permeate fluxes obtained during experiments on the metals wastewater (Figure 4(c)). Although the particles present have a tendency to aggregate due to instability, surface-particle interaction and applied TMP negated the effects of hydrodynamic forces on the larger particles formed. Suspended particles commonly made up of dirt and beverage pigments rapidly deposit on the membrane surface. The deposited particles are then continuously compressed resulting in low membrane porosity (Figures 8(a) and 8(b)) and permeate flux. Such a scenario was also observed at a TMP of 0.4 MPa – although permeate fluxes obtained were slightly higher. Of the two UF membranes used, the JW membrane showed slightly lower flux decline rates (Figure 4(c)).

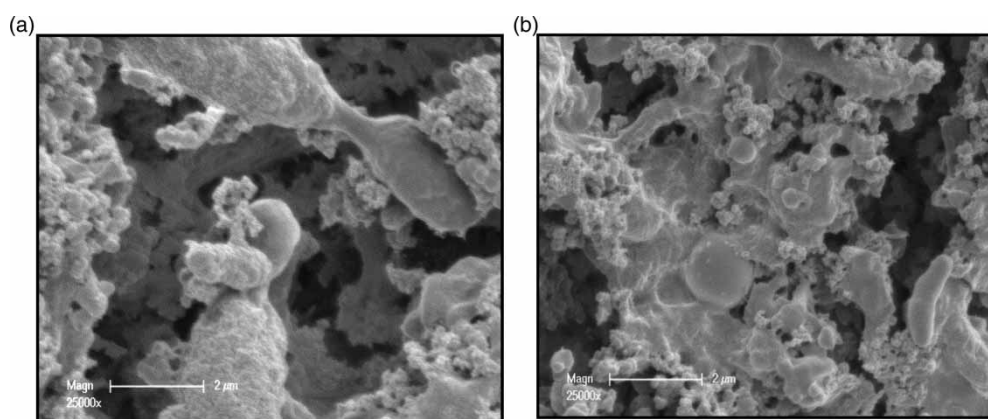


Figure 7 | Surface images of (a) JW and (b) MW membranes used for metals wastewater sample.

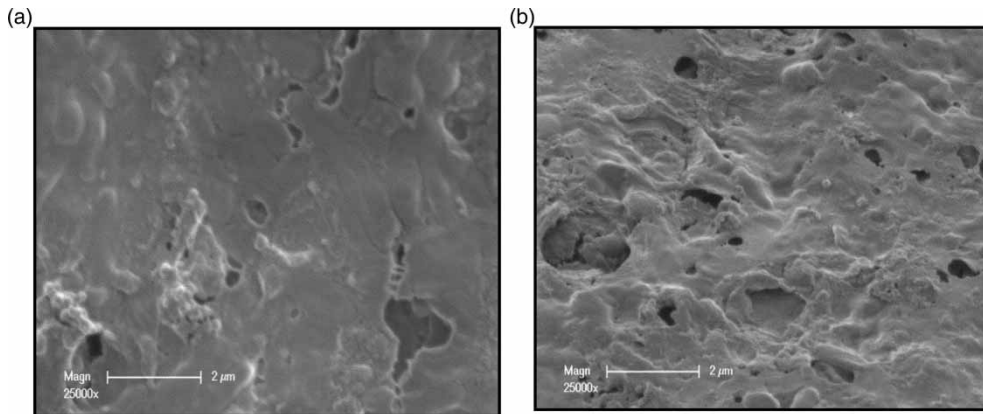


Figure 8 | Surface images of (a) JW and (b) MW membranes used for beverage production wastewater sample.

In general, the fouling mechanisms involved can be deduced as being a combination of intermediate pore blocking and cake layer formation. Deposition of suspended particles happens initially on the membrane pores and was followed by accumulation of particles on the membrane surface.

Turbidity and O&G reduction rates obtained for both the JW and MW membranes show minimal variations (Figures 9(a)–9(c)). In general, for all types of wastewater samples used, both membranes achieved turbidity reduction rates of above 98%. Likewise, both membranes also achieved 100% removal of O&G for all wastewater samples used. In terms of TOC reduction, the performance of the two membranes varied with TMP. When evaluated on the oily wastewater sample, the JW membrane's TOC reduction rate appeared to increase with an increase in TMP, while the MW membrane's TOC reduction rate appeared to decrease with an increase in TMP (Figure 9(a)). Although these experiments were not performed in replicate, such a TOC rejection characteristic, as exhibited by the MW membrane for an oily wastewater sample, is consistent with the results obtained by Akdemir & Ozer (2009). On the other hand, when the membranes were evaluated on the metals and beverage production wastewater samples, TOC reduction rates for both membranes appeared to show a slight increase when the TMP was increased from 0.2 to 0.4 MPa (Figures 9(b) and 9(c)). Notably, the highest TOC reduction for both membranes was obtained from UF experiments involving the beverage production wastewater sample, the TOC reduction rates being above 80%, suggesting that most of the TOC content

of the beverage production wastewater may be associated with suspended solids.

NF and RO experiments

Similar to the UF experiments, the permeate fluxes for both the NF and RO membranes were calculated using Equation (2). To account for temperature variations, all permeate fluxes were standardized at a temperature of 25 °C using Equation (4):

$$J_{25^{\circ}\text{C}} = J/\text{TCF} \quad (4)$$

where $J_{25^{\circ}\text{C}}$ is the flux at a standard temperature of 25 °C ($\text{m}^3 \text{m}^{-2} \text{s}^{-1}$), J is the actual flux measured ($\text{m}^3 \text{m}^{-2} \text{s}^{-1}$) and TCF is the temperature correction factor (dimensionless). The TCF can be estimated using Equation (5) (Crittenden et al. 2005):

$$\text{TCF} = (1.03)^{T_M - 25} \quad (5)$$

where T_M is the measured temperature (°C).

For the three different wastewater types, the permeate fluxes obtained for the RO (AK) membrane at different TMPs are shown in Figures 10(a)–10(c). In general, as the TMP increased, significant improvements in permeate fluxes were measured for all types of wastewater samples used. The highest permeate fluxes were measured for the beverage production wastewater whilst the lowest permeate

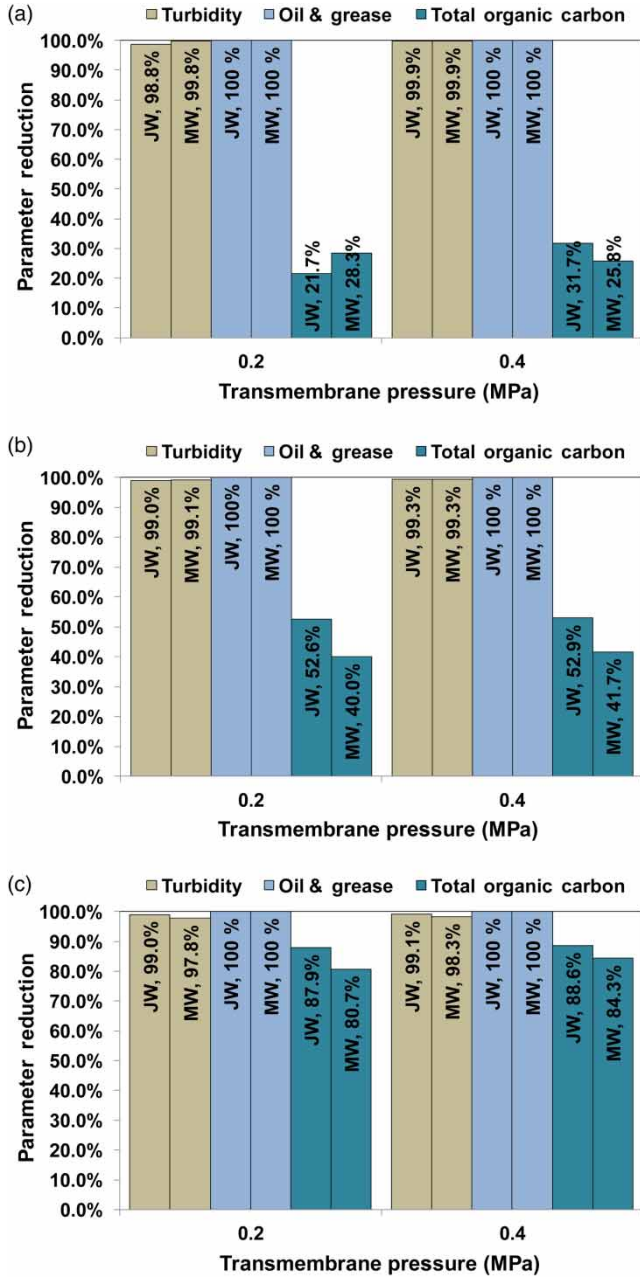


Figure 9 | Performance of the JW and MW membranes on the reduction of water quality parameters such as turbidity, O&G and TOC: (a) oily wastewater sample; (b) metals wastewater sample; (c) beverage production wastewater sample.

fluxes were measured for the metals wastewater sample (car manufacturer).

It is proposed that the low permeate fluxes obtained for the metals wastewater sample could be due to metal oxide fouling. The metals wastewater sample contains elevated concentrations of heavy metals, including Fe, Mn, Ni and

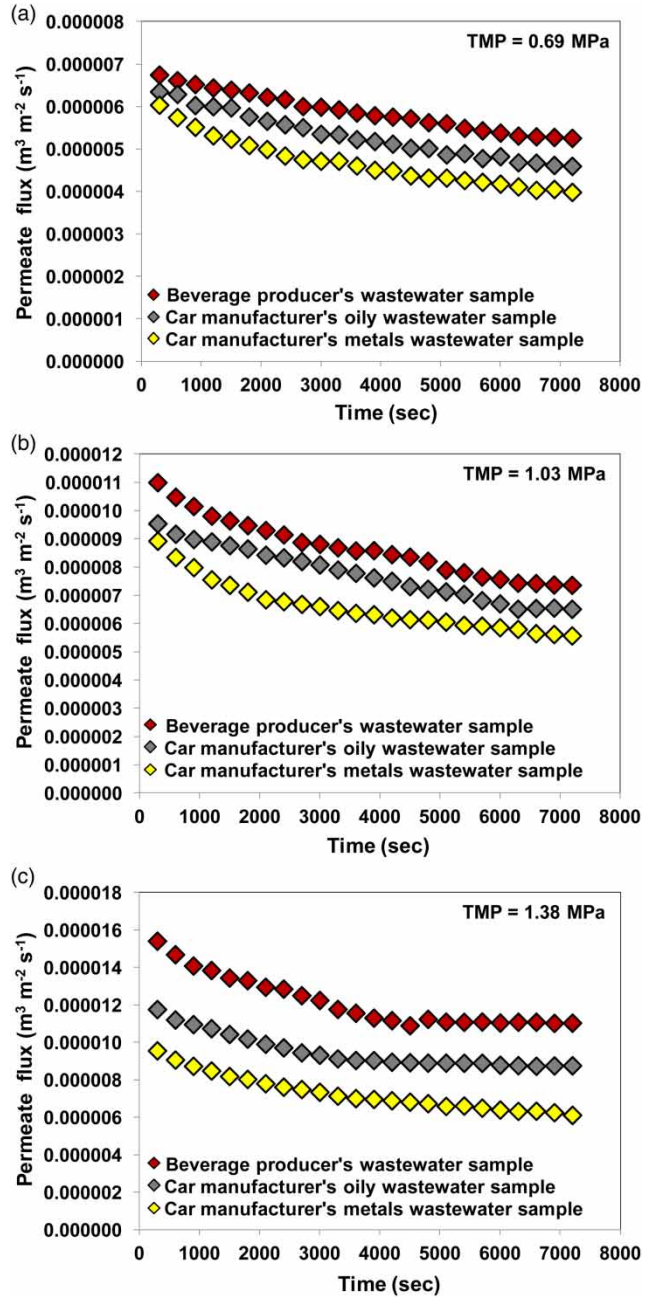


Figure 10 | Permeate fluxes obtained for RO (AK) membrane for different wastewater samples used.

Zn (Table 2). Fe, in particular, is known to be susceptible to oxidation (Crittenden *et al.* 2005) and since the experimental apparatus (Figure 1) is a closed loop system, the flow of the concentrate back into the feed tank promotes rapid mixing of the wastewater sample. This rapid mixing is similar to aerating a pond to increase dissolved oxygen

content. As a result, the process may facilitate the formation of insoluble iron and other metal oxides, resulting in the deposition of oxide particles onto the surface of the RO membrane (Figures 11(b) and 11(c)). Such fouling would be expected to be further intensified as the pressure increases (Figure 11(c)).

On the other hand, the highly organic character of the oily and beverage production wastewater samples resulted in relatively higher permeate fluxes for the RO membrane. Such a wastewater characteristic could be considered appropriate for the RO membrane, which is known to be effective in the separation of organic molecules (Pinnekamp & Friedrich 2006). Because these wastewaters mostly contain organic contaminants, less severe membrane fouling might be expected, even at a high TMP of 1.38 MPa, and this is apparent from the electron micrographs shown in Figures 12(a) and 12(b). Aside from higher permeate fluxes, the RO membrane used also had high conductivity

and COD reduction rates. For the oily wastewater sample, conductivity and COD reduction rates were more than 96.0 and 98.0% respectively. For the beverage production wastewater sample, conductivity and COD reduction rates were both more than 98.0%. Conductivity and COD reduction rates for both the beverage production and oily wastewater samples appeared to be dependent on applied TMP (Figures 13(a) and 13(b)).

An NF (DL series) membrane was also evaluated with respect to the metals wastewater sample since this type of membrane has been reported to be effective in removing heavy metals present in wastewater streams (Ahn *et al.* 1999; Mohammad *et al.* 2004; Qdais & Moussa 2004; Frarès *et al.* 2005). The results of our experiments show that permeate fluxes obtained for the NF membrane were approximately two times higher than the permeate fluxes obtained for the RO membrane (Figures 14(a)–14(c)). The superior performance of the NF membrane for

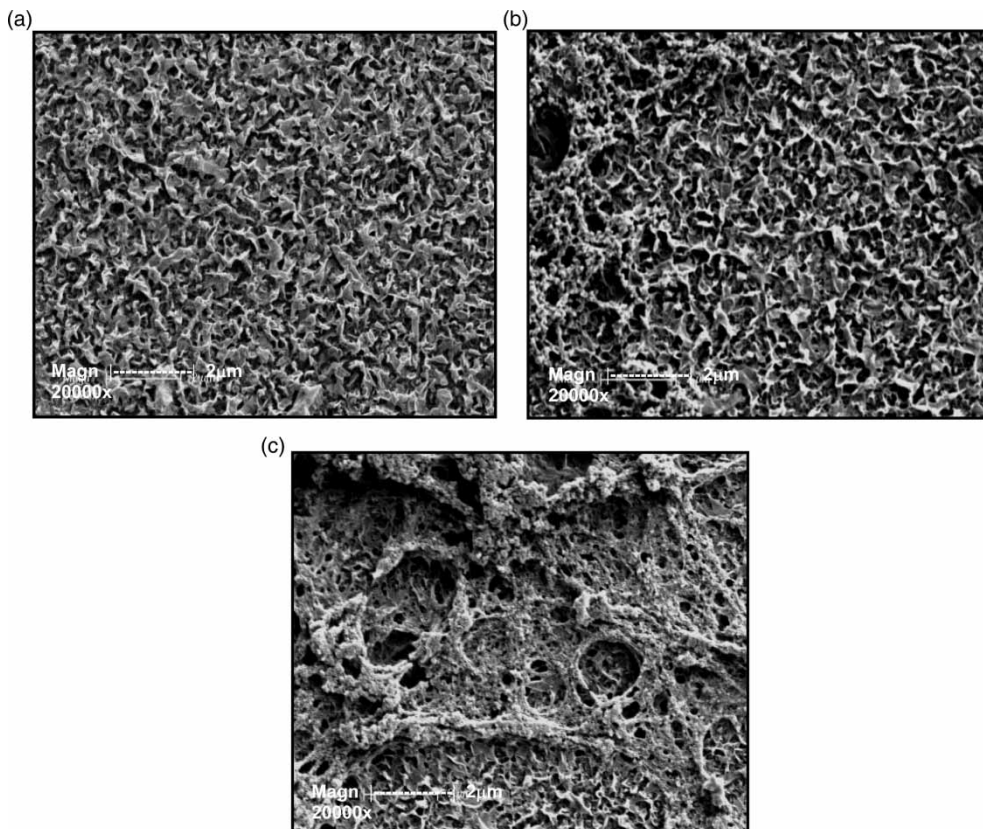


Figure 11 | Surface structure of (a) fresh AK membrane, (b) AK membrane used for metals wastewater sample at 0.69 MPa and (c) AK membrane used for metals wastewater sample at 1.38 MPa.

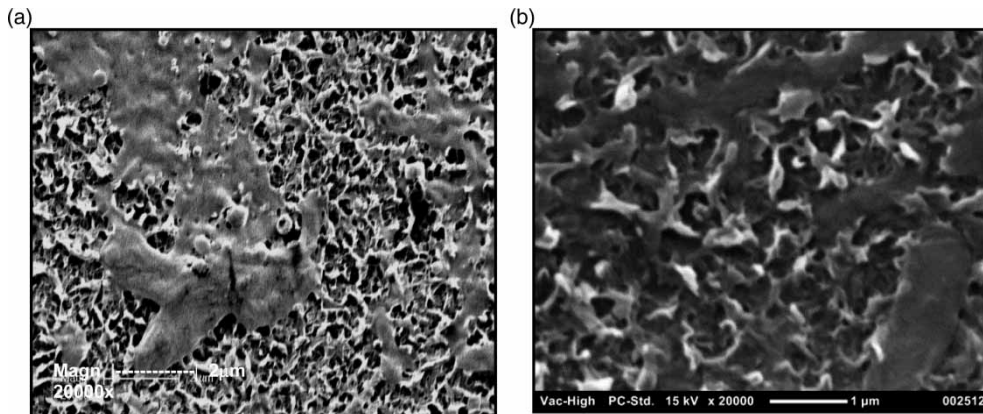


Figure 12 | Surface structure of (a) AK membrane used for oily wastewater sample at 1.38 MPa and (b) AK membrane used for beverage production wastewater sample at 1.38 MPa.

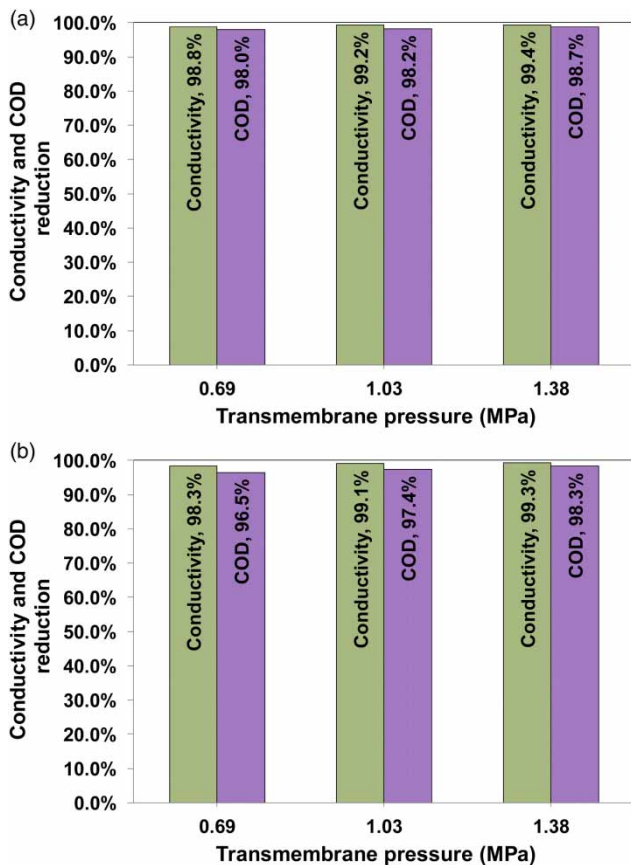


Figure 13 | Conductivity and COD reduction rates of RO (AK) membrane for (a) beverage production wastewater sample and (b) oily wastewater sample.

the metals wastewater sample can be attributed to its separation mechanism. Unlike an RO membrane, whose primary separation mechanism is solution-diffusion, an NF membrane combines solution-diffusion and charge

repulsion mechanisms to separate dissolved organic molecules and polyvalent inorganic ions (Mohammad *et al.* 2004; Pinnekamp & Friedrich 2006). The inherent charge on the NF membrane's surface would be expected to facilitate the rejection of similarly charged solutes. Likewise, because of this surface charge, it is also able to effectively reject similarly charged metal species (Mohammad *et al.* 2004) and metal oxide particles present in the metals wastewater sample. Consequently, fouling of the NF membrane due to the formation of insoluble metal oxide particles would be expected to be inhibited. Assuming that the observed deposition on the membrane surface is primarily metal oxide, Figures 15(b) and 15(c) demonstrate that, even at high TMP, the material does not appear to be significantly compressed onto the surface.

The conductivity reduction for both the NF (DL) and RO (AK) membranes for the metals wastewater sample show values of more than 60.0% at all TMPs used (Figure 16(a)). This suggests that a single pass system is not enough if water reclamation is aimed at replacing drinking quality water to be supplied to processes. In terms of COD reduction, the RO membrane appears to have relatively higher reduction rates than the NF membrane (Figure 16(b)). For the RO membrane, COD reduction rates were more than 94.0%, while for the NF membrane, COD reduction was just above 74.0%. In general, conductivity and COD reduction rates were slightly dependent on TMP – as TMP increased, reduction rates slightly increased.

Both NF and RO membranes showed rejection rates of more than 99.0% for the metals Mn, Ni and Zn.

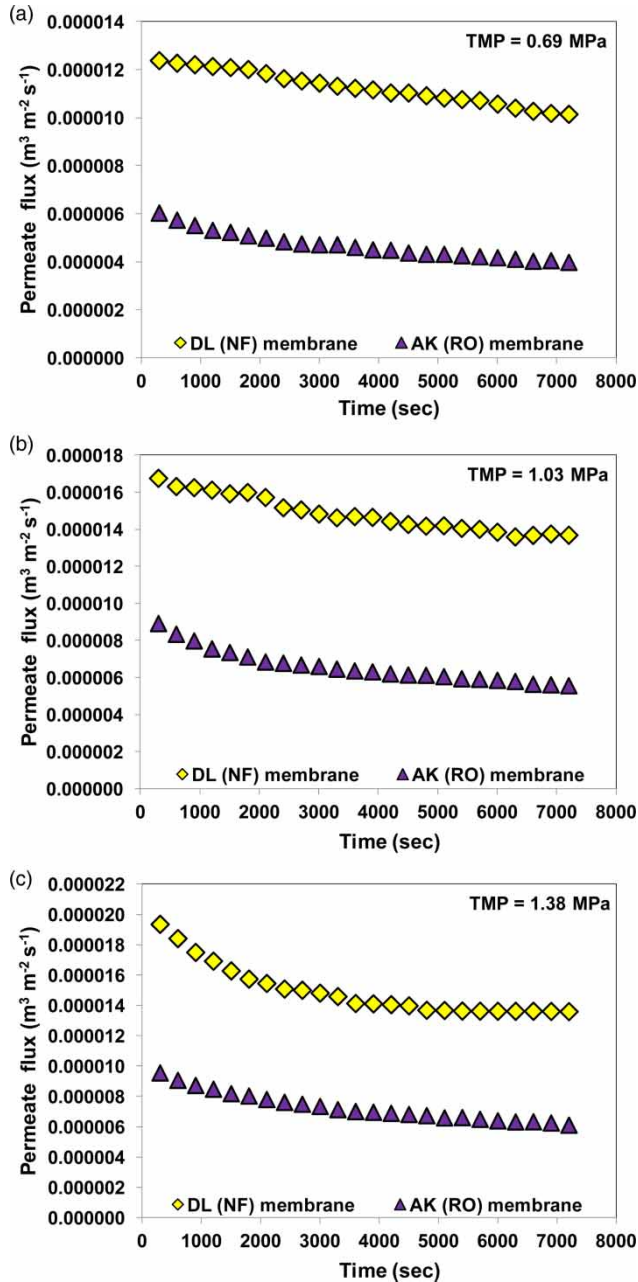


Figure 14 | Permeate fluxes measured for RO (AK) and NF (DL) membranes with respect to metals wastewater sample.

Interestingly, for Fe, the NF membrane had rejection rates of 84.0, 86.2 and 87.5%, and the RO membrane had lower rejection rates – 58.3, 59.6 and 62.2%, respectively, at TMPs 0.69, 1.03 and 1.38 MPa (Figures 17(a) and 17(b)). The selective passage of Fe through both membranes, although intriguing, has not been investigated further in

this study. However, it is tempting to relate this to the fact that the Fe is likely to be trivalent, whereas the other metals are all divalent. The phenomenon might also be related to the relative speciation profiles of the different metals in the wastewater. Additionally, the work conducted by Diallo *et al.* (2013) showed that at high acid concentration, chloride retention is negative – suggesting that electrostatic interactions can have an influence in the transfer mechanism during NF. This result was based on a model solution of iron chloride ($18.6 \times 10^{-3} \text{ mol L}^{-1} \text{ FeCl}_3$) mixed in different concentrations of phosphoric acid (H_3PO_4 : 0.12, 1.2 and 5.9 mol L^{-1}) (Diallo *et al.* 2013).

Energy consumption

In general, improvements in permeate fluxes and reduction/rejection rates of critical water quality parameters were achieved at higher TMPs. However, maintaining higher TMPs usually involve the consumption of substantial amounts of energy, especially for systems requiring larger pumps (Agana *et al.* 2011). To investigate this further at a laboratory-scale level, the average power consumption (P , kW) of the pump motor for each experiment run was recorded. The recorded power consumptions were subsequently used to calculate total energy consumptions (EC_T , kWh) using Equation (6):

$$EC_T = Pt \quad (6)$$

where t is the experiment duration (hours). Tables 3 and 4 show the energy consumption for all the membranes used on specific wastewater samples.

For the UF experiments, minimal increase in energy consumption was obtained when TMP was increased from 0.2 to 0.4 MPa (Table 3). On average, the increase in energy consumption was approximately 2.0%. On the other hand, a significant increase in energy consumption was calculated for the NF and RO experiments. When TMP was increased from 0.69 to 1.03 MPa, an average increase of approximately 18.0% was obtained. Increasing the TMP further to 1.38 MPa resulted in an additional average increase of 18.0%. It is also worth mentioning that the energy consumption of the RO membrane was comparable to the NF membrane during experiments involving the car

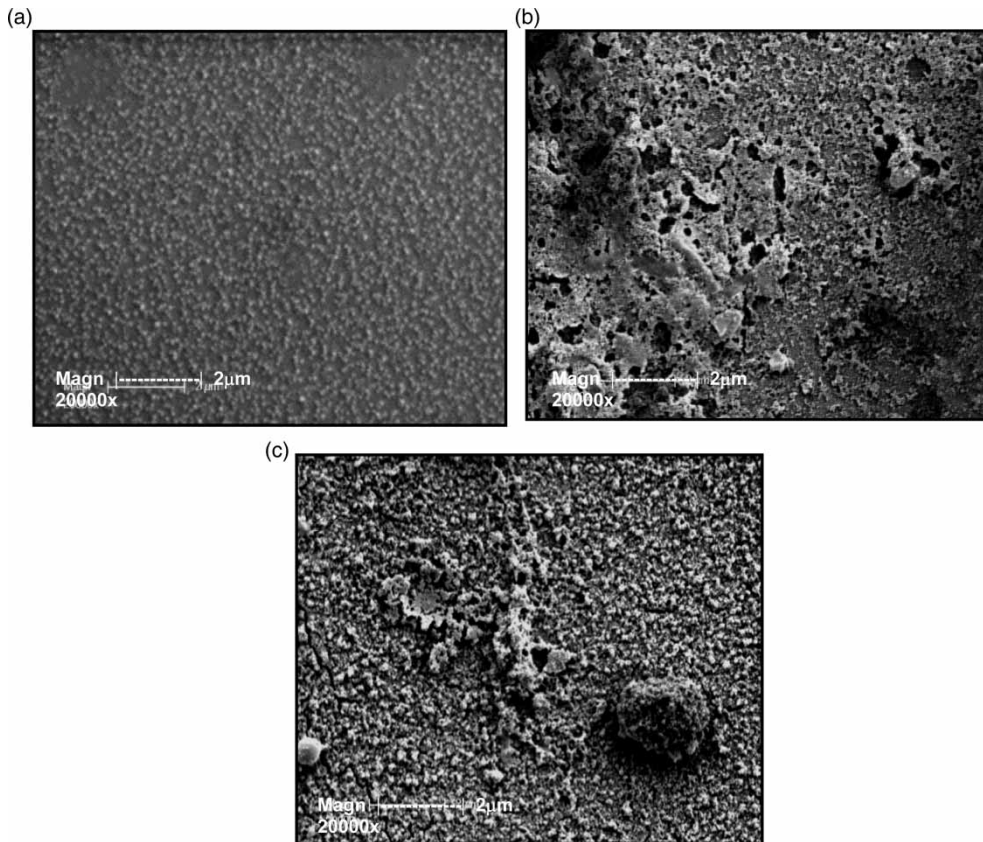


Figure 15 | Surface structure of (a) fresh DL membrane, (b) DL membrane used for metals wastewater sample at 0.69 MPa and (c) DL membrane used for metals wastewater sample at 1.38 MPa.

manufacturer's metals wastewater sample. The low energy consumption of the RO membrane can be attributed to its inherent characteristic of being a low-pressure membrane.

CONCLUSIONS

The above experiments demonstrated the suitability of selected polymeric membranes for the reclamation of different wastewater streams generated by a car manufacturer and a beverage producer. Based on these results, the following conclusions may be drawn:

1. Neither the JW and MW UF membranes can be used directly as pretreatment for the oily wastewater stream due to the presence of suspended CED paint particles. Although particle deposition can be minimized by increasing the CFV, membrane cleaning of the deposited CED paint particles is the main problem. The nature and frequency of cleaning to remove the deposited CED paint particles may significantly degrade the membrane material – leading to a shorter membrane lifespan.
2. Of the two UF membranes tested on the beverage production wastewater stream, the JW membrane proved more suitable for pretreatment than the MW membrane. Flux decline rates for the JW membrane were lower as compared to the MW membrane. Likewise, for this specific wastewater stream, the JW membrane showed higher reduction rates with respect to critical water parameters such as turbidity and TOC.
3. The JW membrane was also suitable for pretreatment of the metals wastewater stream. It showed lower flux decline rates and higher turbidity and TOC reduction rates compared to the MW membrane.
4. The RO (AK) membrane was suitable for use in the reclamation of two wastewater streams – the oily and beverage production wastewaters. Fouling rates

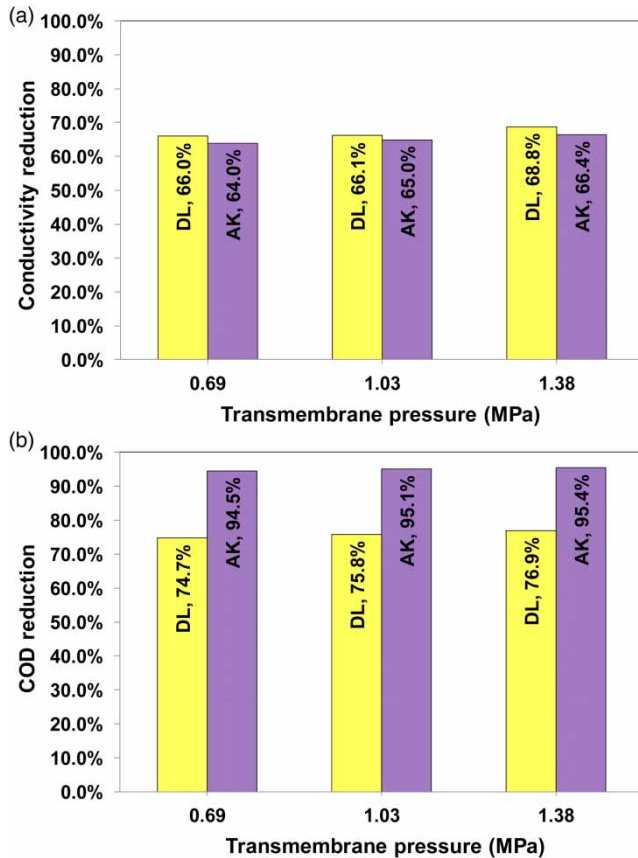


Figure 16 | (a) Conductivity and (b) COD reduction rates of NF (DL) and RO (AK) membranes with respect to metals wastewater sample.

of the RO membrane at these two wastewater streams were slow as reflected by the permeate flux decline rates. Furthermore, reduction rates of critical water quality parameters such as conductivity and COD were high.

- The NF (DL) membrane was more suitable than the RO (AK) membrane for the reclamation of the metals wastewater stream. Permeate fluxes obtained for the NF membrane at all TMPs used was significantly higher compared to the RO membrane. In terms of metals rejection, the NF membrane generally had higher metals rejection rates than the RO membrane. Although the NF membrane had relatively higher permeate fluxes, its conductivity and COD reduction rates were just above 66.0 and 74.0% respectively. Therefore, the use of a single pass system is not sufficient if reclaimed water is intended for processes requiring drinking quality water (water supplied by a local water utility).

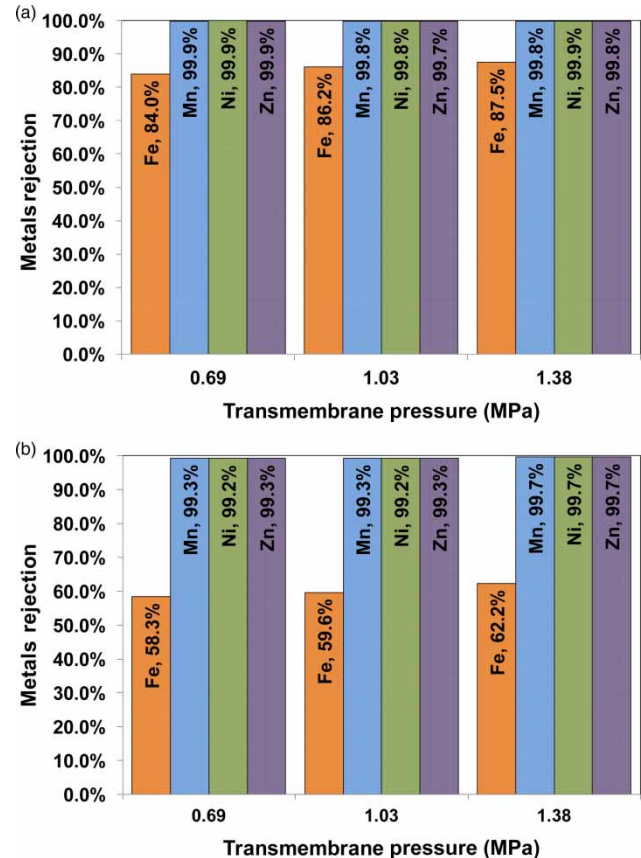


Figure 17 | Metals rejection rates of (a) NF (DL) and (b) RO (AK) membranes with respect to metals wastewater sample.

Table 3 | Energy consumptions for UF experiments

Sample	JW		MW	
	Energy consumption, kWh			
	0.2 MPa	0.4 MPa	0.2 MPa	0.4 MPa
Car manufacturer's oily wastewater	0.112	0.114	0.112	0.114
Car manufacturer's metals wastewater	0.110	0.112	0.110	0.112
Beverage producer's wastewater	0.110	0.114	0.110	0.114

- Not unexpectedly, the energy consumptions for all the membranes used were dependent on TMP: as TMP increased, energy consumption also increased. It was found that energy consumption of the RO membrane was comparable to the energy consumption of the NF

Table 4 | Energy consumptions for NF and RO experiments

Sample	DL			AK		
	Energy consumption, kWh					
	0.69 MPa	1.03 MPa	1.38 MPa	0.69 MPa	1.03 MPa	1.38 MPa
Car manufacturer's oily wastewater	–	–	–	0.202	0.236	0.276
Car manufacturer's metals wastewater	0.200	0.238	0.286	0.200	0.240	0.280
Beverage producer's wastewater	–	–	–	0.206	0.238	0.278

membrane. The slightly lower energy consumption of the RO membrane can be attributed to its inherent characteristic of being a low-pressure membrane.

REFERENCES

- Agana, B. A., Reeve, D. & Orbell, J. D. 2011 Optimization of the operational parameters for a 50 nm ZrO₂ ceramic membrane as applied to the ultrafiltration of post-electrodeposition rinse wastewater. *Desalination* **278**, 325–332.
- Agana, B. A., Reeve, D. & Orbell, J. D. 2012 The influence of an applied electric field during ceramic ultrafiltration of post-electrodeposition rinse wastewater. *Water Res.* **46**, 3574–3584.
- Ahn, K. H., Song, K. G., Cha, H. Y. & Yeom, I. T. 1999 Removal of ions in nickel electroplating rinse water using low-pressure nanofiltration. *Desalination* **122**, 77–84.
- Akdemir, E. O. & Ozer, A. 2009 Investigation of two ultrafiltration membranes for treatment of olive oil mill wastewater. *Desalination* **249**, 660–666.
- Anderson, J. E., Springer, W. S. & Strossberg, G. G. 1981 Application of reverse osmosis to automotive electrocoat paint wastewater recycling. *Desalination* **36**, 179–188.
- ASTM (American Society for Testing and Materials) 1985 Zeta Potential of Colloids in Water and Waste Water. ASTM Standard D 4187-82.
- Crittenden, J. C., Trussell, R. R., Hand, D. W., Howe, K. J. & Tchobanoglous, G. 2005 *Water Treatment: Principles and Design*. 2nd edn. John Wiley & Sons, Inc., Hoboken, NJ.
- Diallo, H., Rabiller-Baudry, M., Khaless, K. & Chaufer, B. 2013 On the electrostatic interactions in the transfer mechanisms of iron during nanofiltration in high concentrated phosphoric acid. *J. Membr. Sci.* **427**, 37–47.
- Frarès, N. B., Taha, S. & Dorange, G. 2005 Influence of the operating conditions on the elimination of zinc ions by nanofiltration. *Desalination* **185**, 245–253.
- GEC (General Electric Company) 2010 GE Water and Process Technologies: MW Series Fact Sheet. http://www.gewater.com/pdf/Fact%20Sheets_Cust/Americas/English/AM-FSpwMWSeries_EN.pdf (accessed 16 December 2011).
- Howe, K. J., Marwah, A., Chiu, K.-P. & Adham, S. S. 2007 Effect of membrane configuration on bench-scale MF and UF fouling experiments. *Water Res.* **41**, 3842–3849.
- Jezowska, A., Schipolowski, T. & Wozny, G. 2006 Influence of simple pre-treatment methods on properties of membrane material. *Desalination* **189**, 43–52.
- Mänttari, M., Pihlajamäki, A., Kaipainen, E. & Nyström, M. 2002 Effect of temperature and membrane pre-treatment by pressure on the filtration properties of nanofiltration membranes. *Desalination* **145**, 81–86.
- Mohammad, A. W., Othaman, R. & Hilal, N. 2004 Potential use of nanofiltration membranes in treatment of industrial wastewater from Ni-P electroless plating. *Desalination* **168**, 241–252.
- Mohammadi, T. & Esmaelifar, A. 2004 Wastewater treatment using ultrafiltration at a vegetable oil factory. *Desalination* **166**, 329–337.
- Pinnekamp, J. & Friedrich, H. (eds) 2006 *Municipal Water and Waste Management: Membrane Technology for Waste Water Treatment*. 2nd edn. FiW VERLAG, Aachen, vol. 2.
- Qdais, H. A. & Moussa, H. 2004 Removal of heavy metals from wastewater by membrane processes: A comparative study. *Desalination* **164**, 105–110.
- Qin, J.-J., Wong, F.-S., Li, Y.-Q., Nyunt, M. & Lian, Y.-T. 2004 The use of ultrafiltration for treatment of spent solvent cleaning rinses from nickel-plating operations: membrane material selection study. *Desalination* **170**, 169–175.
- Streitberger, H. 2007 Electrodeposition coatings. In: *Automotive Paints and Coatings* (H. Streitberger & K. Dossel, eds). 2nd edn, Wiley-VCH, Weinheim, pp. 89–127.
- Tay, J.-H. & Jeyaseelan, S. 1995 Membrane filtration for reuse of wastewater from beverage industry. *Resour. Conserv. Recyc.* **15**, 33–40.
- Wang, Z. G., Wan, L. S. & Xu, Z. K. 2007 Surface engineering of polyacrylonitrile-based asymmetric membranes towards biomedical applications: An overview. *J. Membr. Sci.* **304**, 8–23.

First received 30 January 2013; accepted in revised form 2 May 2013. Available online 17 July 2013